ACS MEASUREMENT SCIENCE Au
AN OPEN ACCESS JOURNAL OF THE AMERICAN CHEMICAL SOCIETY

pubs.acs.org/measureau

Article

Simultaneous Measurement of Striatal Dopamine and Hydrogen Peroxide Transients Associated with L-DOPA Induced Rotation in Hemiparkinsonian Rats

Leslie R. Wilson,[#] Christie A. Lee,[#] Catherine F. Mason, Sitora Khodjaniyazova, Kevin B. Flores, David C. Muddiman, and Leslie A. Sombers*

Cite This: *ACS Meas. Sci. Au* 2022, 2, 120−131

Read Online

ACCESS | Metrics & More | Article Recommendations | Supporting Information

ABSTRACT: Parkinson's disease (PD) is a neurodegenerative disorder commonly treated with levodopa (L-DOPA), which eventually induces abnormal involuntary movements (AIMs). The neurochemical contributors to these dyskinesias are unknown; however, several lines of evidence indicate an interplay of dopamine (DA) and oxidative stress. Here, DA and hydrogen peroxide (H_2O_2) were simultaneously monitored at discrete recording sites in the dorsal striata of hemiparkinsonian rats using fast-scan cyclic voltammetry. Mass spectrometry imaging validated the lesions. Hemiparkinsonian rats exhibited classic L-DOPA-induced AIMs and rotations as well as increased DA and H_2O_2 tone over saline controls after 1 week of treatment. By week 3, DA tone remained elevated beyond that of controls, but H_2O_2 tone was largely normalized. At this time point, rapid chemical transients were time-locked with spontaneous bouts of rotation. Striatal H_2O_2 rapidly increased with the initiation of contraversive rotational behaviors in lesioned L-DOPA animals, in both hemispheres. DA signals simultaneously decreased with rotation onset. The results support a role for these striatal neuromodulators in the adaptive changes that occur with L-DOPA treatment in PD and reveal a precise interplay between DA and H_2O_2 in the initiation of involuntary locomotion.

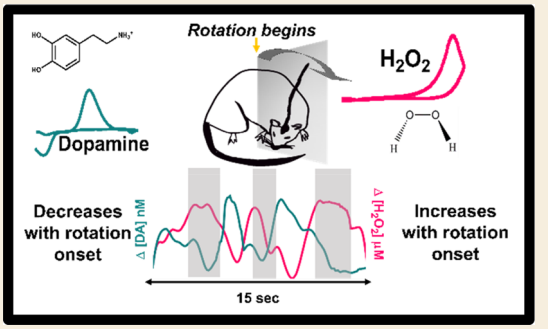

KEYWORDS: *fast-scan cyclic voltammetry, oxidative stress, Parkinson's disease, dyskinesia, IR-MALDESI, mass spectrometry imaging, in vivo, 6-OHDA*

INTRODUCTION

Worldwide, there are ∼10 million people diagnosed with Parkinson's disease (PD),[1] a neurodegenerative disorder that results in muscle rigidity, slowed movement, and resting tremor. Pathologically, PD is marked by the extensive loss of nigrostriatal dopamine (DA) neurons in the substantia nigra pars compacta (SNpc) which innervate the dorsal striatum, a region involved in action selection, locomotion, and habit formation.[2−4] There is no specific known cause for idiopathic PD; however, multiple lines of evidence implicate oxidative stress as an underlying factor in both the initiation and progression of the disease.[5] For instance, decreased mitochondrial complex I activity is evident in postmortem PD tissue[6] and is a common feature of many of the neurotoxin-induced experimental models of PD.[7] This results in enhanced generation of reactive oxygen species (ROS) such as superoxide, hydrogen peroxide (H_2O_2), and hydroxyl radical.[8] H_2O_2 is particularly interesting because it is relatively stable and can accumulate to significant concentrations, allowing it to serve distinct biological roles in signaling and in energy metabolism. In excess, it can lead to deleterious cellular toxicity (oxidative stress).[9]

Dopaminergic replacement therapy with L-DOPA (levodopa; L-3,4-dihydroxyphenylalanine), the metabolic precursor to DA, is a standard treatment that can initially alleviate hypokinetic symptoms of PD. Remarkably little is known about how the dynamics of DA release events change to preserve motor control in PD or how these dynamics are modified during L-DOPA replacement therapy. About 40% of patients undergoing this therapy develop hyperkinetic, involuntary dyskinesias after about 4−6 years of treatment.[10] Eventually, nearly all patients on L-DOPA acquire these involuntary motor complications,[11] which can be as debilitating as PD itself, limiting the long-term therapeutic benefit of L-DOPA.

Studies in unilaterally lesioned animal models indicate that surviving DA neurons can functionally compensate for the

Received: August 13, 2021
Revised: October 21, 2021
Accepted: October 21, 2021
Published: November 8, 2021

https://doi.org/10.1021/acsmeasuresciau.1c00030
ACS Meas. Sci. Au 2022, 2, 120−131

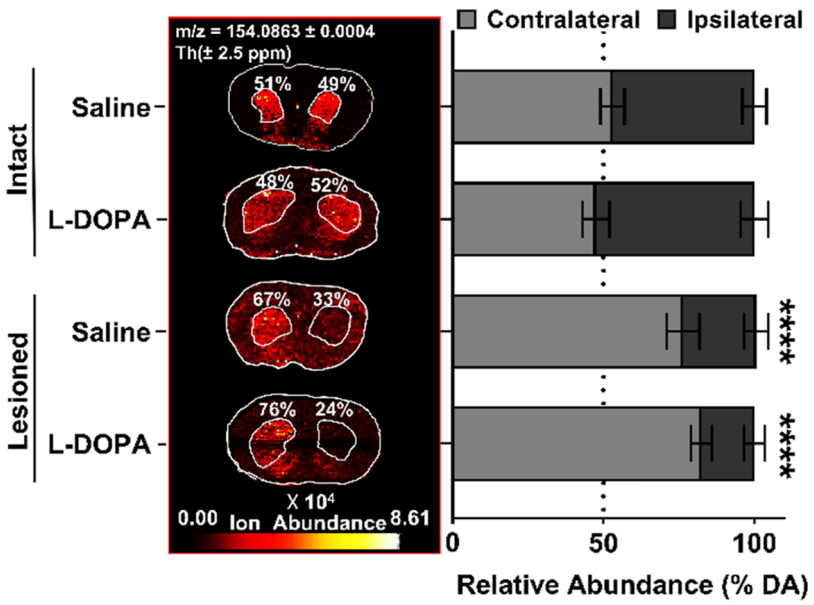

Figure 1. IR-MALDESI MSI was used to quantify relative DA abundance in the dorsal striatum. Left: Representative images (coronal brain slices) for intact and unilaterally 6-OHDA-lesioned rats (measured in Thompsons (Th)). Right: Relative DA abundance was plotted for all treatment groups with 50% indicated by the dashed line. Less DA was measured in the striatum ipsilateral to the lesion (n = 3−4). Asterisks indicate significant differences in comparing contra- *vs* ipsilateral striata for each treatment group (****P < 0.0001).

progressive loss of SNpc DA neurons by up-regulating DA release,[12] which is further augmented by L-DOPA treatment. Striatal DA levels are increased in dialysate collected from the 6-hydroxydopamine (6-OHDA) rat model of PD while the animals are exhibiting L-DOPA-induced abnormal involuntary movements (AIMs) and robust rotations.[13,14] Excess DA can act at subsets of medium spiny neurons (MSNs) to elicit dyskinetic movements.[15] It has been shown that MSN activity leads to the rapid generation of H_2O_2[16] and this can downregulate DA release by way of K_{ATP} channels.[17] However, rapid fluctuations in DA or H_2O_2 ("transients") have not been examined in L-DOPA-treated dyskinetic animals. Thus, many questions remain unanswered regarding the role of these species in the development and expression of dyskinesias.

Fast-scan cyclic voltammetry (FSCV) enables molecules in the brain to be monitored *in situ* with chemical selectivity on the millisecond time scale. It has been used to demonstrate that striatal DA transients are implicated in the modulation of specific behaviors, such as interaction with conspecifics,[18] reward learning,[19−21] and action selection.[4] Although FSCV has been used to simultaneously monitor H_2O_2 and DA in striatal tissue of anesthetized rats,[22] no studies to date have simultaneously measured these neurochemicals at the same recording site in awake, behaving animals. Here, we examine the function of these molecules in the context of movement using a unilaterally 6-OHDA-lesioned rat model treated chronically with L-DOPA. Mass spectrometry imaging (MSI) was used to quantify the relative extent of DA loss by coupling an infrared matrix-assisted laser desorption electrospray ionization (IR-MALDESI) source to a Q Exactive Plus mass spectrometer.[23,24] Hemiparkinsonian rats exhibited well-established AIMs and 360° rotations following L-DOPA administration. Concurrent measurements of striatal H_2O_2 and DA indicate an overall increase in bilateral H_2O_2 and ipsilateral DA tone after 1 week of L-DOPA. At this time, examination of rapid neurochemical dynamics revealed no clear relationship with AIMs (dyskinetic behavior) or the onset of rotation. After 3 weeks of L-DOPA treatment, striatal H_2O_2 tone was largely normalized but ipsilateral DA tone remained generally elevated during dyskinetic behaviors. Interestingly, a rapid increase in H_2O_2 concentration was recorded precisely with the onset of robust rotation, as DA concentrations at the same site simultaneously *decreased*. These unanticipated and novel results advance our understanding of the neuromodulatory role played by H_2O_2 in the brain and provide a new perspective on the function of striatal DA signaling in the context of movement.

RESULTS

IR-MALDESI MSI Validation of the Dopaminergic Lesion

Animals were treated daily for 3 weeks with saline or L-DOPA (6 mg/kg, i.p.), and the relative abundance of DA in dorsal striata was assessed using IR-MALDESI MSI to validate the model. Figure 1 shows representative images for intact controls and unilaterally 6-OHDA-lesioned rats, with relative striatal DA abundance quantified for each treatment group. Overall, two-way ANOVA analysis (hemisphere, $F_{1,16}$ = 75.80, P < 0.0001; treatment, $F_{3,16}$ = 0.0025, P = 0.999; hemisphere × treatment interaction, $F_{3,16}$ = 25.65, P < 0.0001) indicates that DA abundance significantly differed across hemisphere in lesioned animals (ipsilateral *vs* contralateral, P < 0.0001 in both groups) but not in intact controls. Specifically, in L-DOPA-treated hemiparkinsonian animals, DA abundance in the lesioned striatum was only 18 ± 3% of the total DA abundance measured across both striata (n = 4). Similarly, the lesioned striatum of saline-treated rats contained only 24 ± 4% of the abundance attributable to DA (n = 4). Importantly, L-DOPA treatment did not significantly change the relative abundance of DA remaining in lesioned rats when compared to lesioned animals administered saline (P > 0.9987).

Evaluation of Dyskinetic Behaviors

Global AIMs and 360° rotations were not observed (*i.e.*, 0 values) in control groups (lesioned + saline, intact + L-DOPA,

https://doi.org/10.1021/acsmeasuresciau.1c00030
ACS Meas. Sci. Au 2022, 2, 120−131

intact + saline). Therefore, these groups were pooled for behavioral analysis. Control animals mostly rested during the recording sessions, with little ambulation or exploration (Figure 2; behavioral scores at week 1 (black, gray) and

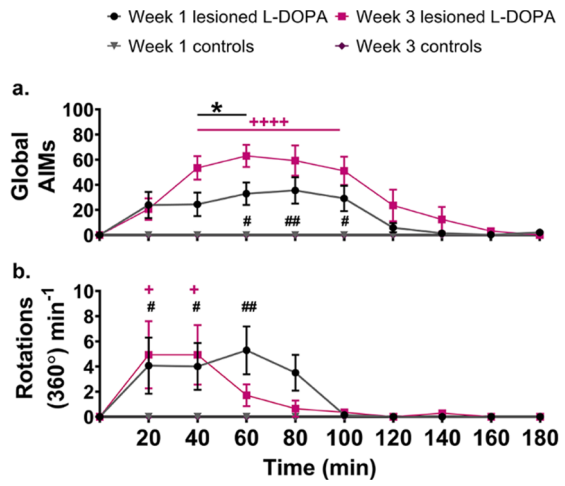

Figure 2. Quantification of dyskinetic behavior. (a) After 1 week of L-DOPA administration (6 mg/kg), lesioned rats exhibited AIMs that differed from baseline (0 min). These peaked 60−100 min after drug administration ($^{\#}P < 0.05$, $^{\#\#}P < 0.01$). After 3 weeks of L-DOPA, dyskinetic movements increased and were evident for a longer duration (40−100 min, $^{++++}P < 0.0001$). The total score for global AIMs increased from week 1 to week 3 after daily L-DOPA treatment ($^{*}P < 0.05$). (b) The number of rotations (360°, per min) increased compared to baseline (0 min) in both week 1 (20−60 min, $^{\#}P < 0.05$, $^{\#\#}P < 0.01$) and week 3 (20 and 40 min, $^{+}P < 0.05$). For both weeks, $n = 7$.

week 3 (magenta, purple)). By contrast, three-way ANOVA indicated that hemiparkinsonian animals exhibited more global AIMs (time × week × treatment interaction $F_{9,135} = 3.175$, $P = 0.0016$) and 360° rotations (time × week × treatment interaction $F_{9,135} = 1.953$, $P = 0.0496$) at an increased frequency (per minute) after both 1 and 3 weeks of L-DOPA treatment (statistical summary in Table S1).

A detailed two-way ANOVA analysis of the AIMs exhibited by lesioned L-DOPA-treated animals ($n = 7$) across a 185 min evaluation period at week 1 (black) *vs* week 3 (magenta) revealed an effect of time ($F_{9,54} = 14.98$, $P < 0.0001$) but not of week ($F_{1,6} = 3.389$, $P = 0.1152$). Notably, there was a significant interaction of time × week ($F_{9,54} = 2.159$, $P = 0.0397$). AIM behavior was significantly increased above baseline (time 0) at 60 min ($P = 0.0044$), 80 min ($P = 0.0018$), and 100 min ($P = 0.0158$) after 1 week of L-DOPA administration (Figure 2a). This is consistent with the time course of AIMs evoked by L-DOPA treatment in prior rodent studies.[25] After 3 weeks of L-DOPA, AIM behavior increased earlier (at 40 min, $P < 0.0001$; 60−100 min, $P < 0.0001$), with global AIM scores being higher than week 1 scores at both 40 min ($P = 0.0189$) and 60 min ($P = 0.0132$) (Figure 2a).

Analysis of 360° rotations (Figure 2b) across the 185 min evaluation period similarly varied with time ($F_{9,54} = 5.789$, $P < 0.0001$) but not with the week of observation ($F_{1,6} = 0.3281$, $P = 0.5876$), and there was no significant time × week interaction ($F_{9,54} = 1.328$, $P = 0.2445$). In week 1, rotations were elevated 20 min ($P = 0.0291$), 40 min ($P = 0.0339$), and 60 min ($P = 0.0018$) after L-DOPA administration. By week 3, the duration of the drug effect on rotations was shorter than that recorded in week 1, consistent with other reports.[26,27] A significant increase in rotation was evident only at 20 min ($P = 0.0042$) and 40 min ($P = 0.0042$).

The extent of the lesion (Figure 1) did not correlate with either the sum of the AIM scores (axial, orolingual, limb) or the total number of 360° rotations recorded in week 1 (Figure S1, black; a, AIMs: $R^2 = 0.132$; b, rotations: $R^2 = 0.035$), as assessed using linear regression analysis. After 3 weeks of L-DOPA treatment, however, the extent of the lesion moderately correlated with the AIMs scores (Figure S1a, pink; $R^2 = 0.825$).

Neurochemical Tone during Dyskinetic Behavior

As the first metric to quantify chemical signaling using bilateral voltammetric recordings in the dorsal striatum, DA and H_2O_2 *tone* were simultaneously monitored. Here, "tone" denotes a slowly graded change in an individual chemical signal, as opposed to the rapid transients typically measured with FSCV. Tone was roughly quantified by calculating the area under the respective concentration *vs* time trace in 300 s bins, normalized to the subject's baseline. In the representative color plot shown in Figure 3a, a mixed signal from both analytes is evident in the same recording (top). The extracted DA (teal, middle) and H_2O_2 (pink, bottom) signals recorded in both striata are graphically presented in Figure 3b−i. Detailed statistics are provided in Table S1, and a representative baseline recording is provided in Figure S4 to demonstrate electrode stability.

After 1 week of L-DOPA (Figure 3 b,d,f,h), baseline-normalized DA and H_2O_2 tone varied in the ipsilateral striatum of hemiparkinsonian animals based on treatment condition ($F_{3,78} = 11.34$, $P < 0.001$ and $F_{3,77} = 10.43$, $P < 0.001$, respectively). Ipsilateral DA tone increased ∼10-fold 100 min after L-DOPA administration (Figure 3b; $P = 0.02$), and H_2O_2 tone was elevated 60−80 min after L-DOPA (Figure 3d; $P = 0.0487$ and $P = 0.0133$) as compared to the intact, L-DOPA-treated controls. Contralaterally, an increase in DA tone was not observed (Figure 3f); however, there was a treatment effect for H_2O_2 tone (Figure 3h; $F_{3,56} = 4.514$, $P = 0.0066$), with a significant elevation over the intact L-DOPA treated group evident 100 min ($P = 0.0408$) after L-DOPA administration.

These L-DOPA induced effects on chemical tone were largely attenuated after 3 weeks of L-DOPA treatment (Figure 3c,e,g,i). In the ipsilateral striatum, DA tone varied with treatment condition ($F_{3,66} = 4.776$, $P = 0.0045$), with L-DOPA treated hemiparkinsonian rats exhibiting increased DA tone 60 min after L-DOPA administration, compared to all control groups (Figure 3c; $P = 0.0075−0.0129$). No changes in DA tone were found in the contralateral striatum (Figure 3g). In the ipsilateral striatum, H_2O_2 tone was normalized by week 3; however, it was slightly elevated in the contralateral striatum (Figure 3i) of lesioned L-DOPA treated rats at one time point (20 min) as compared to intact saline rats ($P = 0.0471$; treatment, $F_{3,67} = 6.003$, $P = 0.0011$). A small elevation in H_2O_2 tone was recorded in the intact L-DOPA-treated rats, as compared to the lesioned L-DOPA-treated group, at 40 min ($P = 0.0186$), 100 min ($P = 0.0354$), and 140 min ($P = 0.0471$).

A Closer Look at Neurochemical Dynamics

A principal advantage of FSCV is that it enables detection of neurochemical dynamics that occur on the second time scale (*transients*). Neither DA nor H_2O_2 transients notably correlated with the expression of individual axial, orolingual or limb AIMs (Figure S2). Figure 4 shows representative voltammetric data collected in the ipsilateral striatum of a

https://doi.org/10.1021/acsmeasuresciau.1c00030
ACS Meas. Sci. Au 2022, 2, 120−131

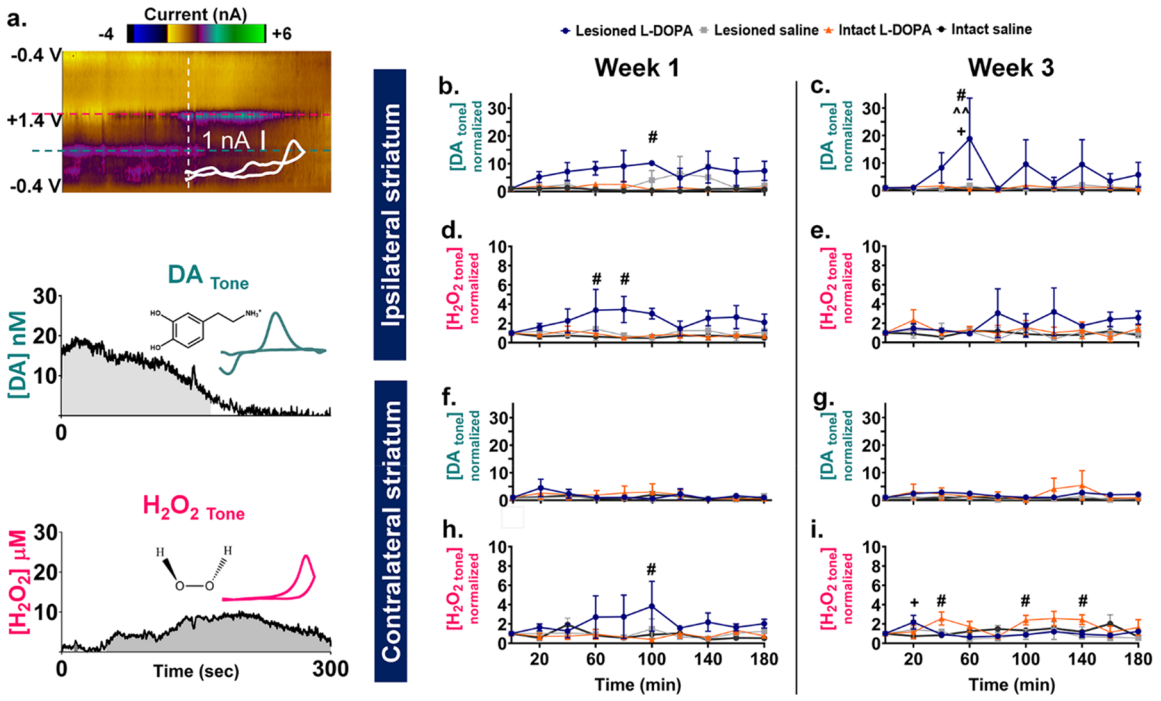

Figure 3. Electrochemical quantification of neurochemical "tone". (a) Top: Representative color plot collected in the ipsilateral striatum of a 6-OHDA lesioned animal 160 min after L-DOPA administration on the 21st day (week 3) of treatment. A mixed H_2O_2 (oxidation at ∼1.4 V, red dashed line) and DA (oxidation at ∼0.6 V, blue dashed line) signal is evident. The CV (inset) was extracted at the time of the vertical dashed line. Bottom: Neurochemical tone (DA: teal, middle; H_2O_2: pink, bottom) was approximated for each species by integrating the area under the respective concentration *vs* time traces. (b,c) In hemiparkinsonian animals treated with L-DOPA (blue), baseline-normalized DA tone increased in the ipsilateral striatum after both 1 and 3 weeks of L-DOPA treatment (at 100 and 60 min, respectively). (d) Ipsilateral H_2O_2 tone was elevated 60−80 min after L-DOPA in week 1, and (e) this normalized by week 3. (f,g) Contralateral DA tone was not altered by L-DOPA treatment compared with other treatment groups. However, (h) after 1 week of L-DOPA, the contralateral H_2O_2 tone was increased at 100 min *vs* intact L-DOPA rats. (i) This effect was attenuated by week 3, but H_2O_2 tone was mildly elevated in intact L-DOPA treated animals 40, 100, and 140 min after L-DOPA administration, as compared to lesioned, L-DOPA treated animals. Sidak posthoc comparisons between treatment groups compared to the lesioned L-DOPA condition, $^{\#}P < 0.05$ *vs* intact L-DOPA (red); $^{\wedge\wedge}P < 0.01$ *vs* lesioned saline (gray); $^{+}P < 0.05$ *vs* intact saline (black). For all treatment groups $n = 3$−4.

hemiparkinsonian rat ∼90 min after L-DOPA administration (week 1). Current *vs* time traces for each analyte are shown in Figure 4a, centered on the onset of a bout of rotation (±1 s). In this instance, DA (teal) and H_2O_2 (pink) dynamics are positively correlated (Spearman's rho (ρ) = 0.66, $P = 0.0011$) around the onset of rotational behavior (shown in gray, time 0).

Overall, a range of inconsistent correlations was recorded across animals in both hemispheres (Figure S3). However, an intriguing relationship was evident in some recordings when evaluating DA and H_2O_2 transients. For instance, the raw data for the entire 300 s recording epoch are shown in Figure 4b (top). The concentration *vs* time traces are shown (middle: DA, teal and H_2O_2, pink), with the data shown in Figure 4a indicated by vertical black box. The periods over which the rat was engaged in rotation for at least 1.7 s are shaded in gray. When the data from these four rotational bouts are averaged around the onset of rotation, DA and H_2O_2 are clearly negatively correlated around rotation onset (Figure 4b, bottom, inset; $\rho = -0.84$, $P < 0.0001$). Across all animals, however, DA and H_2O_2 concentrations were positively correlated with respect to one another (Figure 4c, $\rho = 0.5909$, $P = 0.0048$), and there was no consistent trend for either analyte with respect to the initiation of rotational behavior.

By week 3, however, both DA and H_2O_2 transients were time-locked with rotation onset (Figure 5, Video S1). Representative data recorded in the lesioned striatum ∼55−60 min after L-DOPA administration are shown in Figure 5b (top: color plot of raw data, bottom: corresponding concentration *vs* time traces). This recording contains 15 rotational bouts (gray bars) from one hemiparkinsonian subject. Averaged electrochemical data centered on the onset of rotation (±1 s) demonstrate a robust negative correlation between DA (teal) and H_2O_2 (pink) (Figure 5c, bottom; $\rho = -0.9917$, $P < 0.0001$). Interestingly, DA concentrations *decrease* with the onset of rotation as local H_2O_2 concentrations simultaneously *increase* at the same recording site.

Detailed quantification across all rats revealed this striking correlation at nearly all time periods evaluated (Figure 6a−f, top, Figure S5). Shortly after rotations began (∼35−40 min after L-DOPA administration), striatal DA transients were negatively correlated with H_2O_2 concentrations in both hemispheres (Figure 6a, ipsilateral $\rho = -0.6104$, $P = 0.0033$; Figure 6d, contralateral $\rho = -0.98$, $P < 0.0001$). This strong negative correlation remained apparent at ∼55−60 min (Figure 6b, ipsilateral $\rho = -0.99$, $P < 0.0001$; Figure 6e, contralateral $\rho = -0.98$, $P < 0.0001$) and ∼85−90 min after L-DOPA administration, as dyskinesias were subsiding (Figure 6c, ipsilateral $\rho = -0.92$, $P < 0.0001$; Figure 6f, contralateral $\rho = -0.83$, $P < 0.0001$). Cross-correlational analysis of H_2O_2 *vs* DA concentrations (Figure 6a−f, middle and bottom) revealed that changes in DA and H_2O_2 concentrations were negatively correlated precisely at the onset of the rotational behavior

https://doi.org/10.1021/acsmeasuresciau.1c00030
ACS Meas. Sci. Au 2022, 2, 120−131

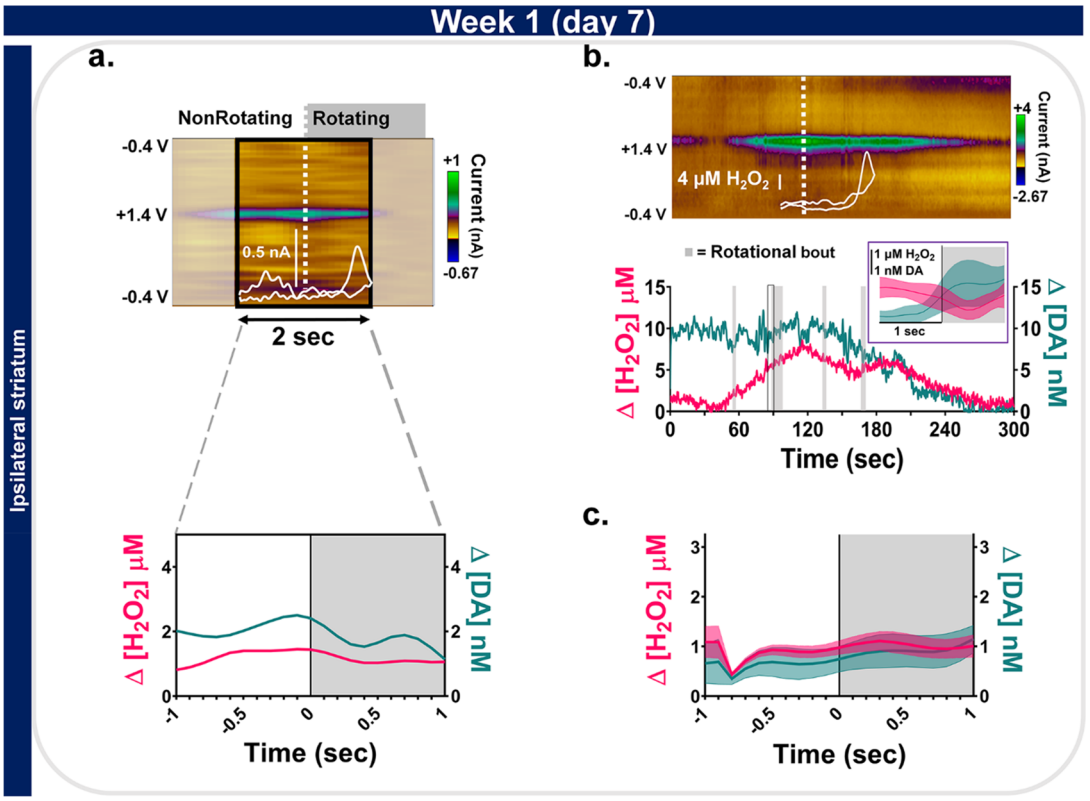

Figure 4. After 1 week of L-DOPA, striatal DA and H_2O_2 transients did not reliably correlate with contraversive rotational behavior. (a) Representative data collected in the lesioned striatum of one animal during one rotational bout ∼85−90 min after L-DOPA administration. Top: Color plot of raw data. Bottom: H_2O_2 (pink) and DA (teal) traces extracted ±1.0 s around the onset of rotation (vertical black box on color plot). Neither signal was notably correlated with rotation onset. (b) Top: color plot of raw data for the entire 300 s epoch from which the representative data in (a) were extracted. Bottom: concentration *vs* time traces for this recording. Four periods of rotational behavior are shaded in gray, and the black vertical box indicates the data shown in (a). Inset: averaged concentration traces from all rotational bouts (n = 4) recorded in this evaluation epoch from this animal. Here, a clear negative correlation was apparent around rotation onset (ρ = −0.84, P < 0.0001). (c) Across all animals (n = 2−3, ipsilateral striatum), DA and H_2O_2 were positively correlated (ρ = 0.5909, P = 0.0048), with no consistent trend noted for either analyte with respect to the initiation of rotational behavior (0 s).

(ipsilateral: Figure 6c, r = −0.259; contralateral: Figure 6d,e with r = −0.258 and r = −0.215, respectively).

DISCUSSION

Rapid extracellular DA transients have not been investigated during the development and expression of dyskinetic movements, and H_2O_2 dynamics have not been measured with precise temporal and spatial resolution, to date, in any freely moving animals. In this study, we used state-of-the-art measurement technologies to quantify DA and H_2O_2 in the dorsal striatum over several weeks of L-DOPA treatment while evaluating the development of AIMs and rotation behavior in unilaterally 6-OHDA-lesioned rats. First, the extent of dopaminergic denervation in the striatum was assessed using IR-MALDESI MSI[23,24] (Figure 1), and this was ultimately correlated with the extent of the L-DOPA induced AIMs and rotational behaviors (Figure S1). Over the course of L-DOPA treatment, real-time DA and H_2O_2 dynamics were concurrently recorded in both the intact and lesioned striata of awake animals using FSCV (Figures 3−6). This represents an important advance in neurochemical monitoring because, to date, studies have been almost entirely limited to recordings of only one analyte (DA), collected using one electrode. The neurochemical signals were then quantitatively assessed during L-DOPA induced AIMs and rotational behavior on both the minutes (Figure 3) and seconds (Figure 4−6) time scale, providing a means to compare the data to the extensive microdialysis literature, as well as important insight into adaptive changes in striatal signaling.

Consistent with previous reports,[28] the 6-OHDA-lesioned rats exhibited severe AIMs (Figure 2a) with contraversive rotations after L-DOPA administration (Figure 2b). By the third week of L-DOPA treatment, the AIMs increased in magnitude compared to the first week[13,29] (Figure 2a). Hemiparkinsonian rats exhibited robust 360° contraversive rotations (Figure 2 b) that began ∼20 min after L-DOPA treatment. These rotations are not a measure of dyskinesia per se, but they do serve as a quantifiable behavior that is useful in evaluating antiparkinsonian efficacy. They are thought to result from asymmetry in dopaminergic circuits after L-DOPA treatment,[30−32] including differences in DA receptor sensitivity across striata.[33] The duration of time over which the rotational bouts were evident decreased overall from the first to the third week of treatment (Figure 2b), consistent with other reports.[27,34] This suggests a sensitized response that occurs simultaneously with a "wearing-off" phenomenon, similar to that reported in human PD studies.[35]

Hemiparkinsonian animals treated with saline exhibited no changes in electrochemically recorded DA or H_2O_2 tone in either hemisphere (as compared to intact controls; Figures 3b−i, gray), consistent with microdialysis studies.[36,37] Conversely, ipsilateral DA and bilateral H_2O_2 tone were elevated

https://doi.org/10.1021/acsmeasuresciau.1c00030
ACS Meas. Sci. Au 2022, 2, 120−131

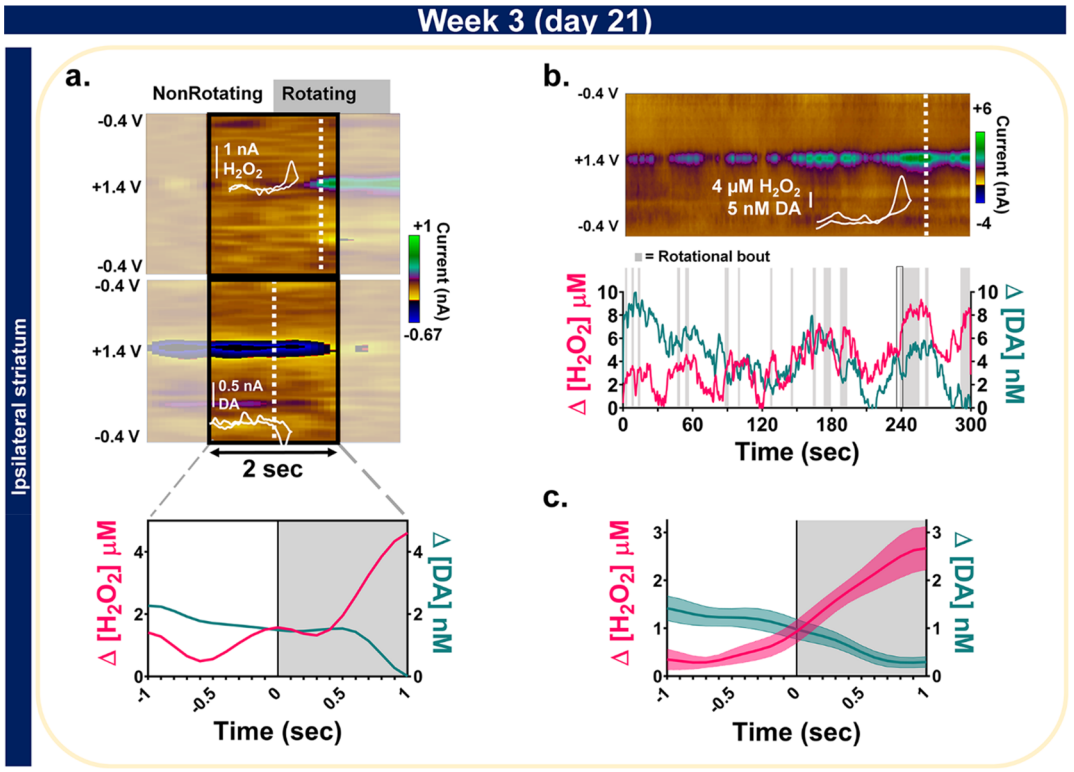

Figure 5. Representative data were collected in the lesioned striatum of one animal after 3 weeks of L-DOPA treatment. (a) Top: Color plot of raw data collected ∼55−60 min after L-DOPA administration, with background subtraction for H_2O_2 (above) and DA (below). Representative voltammograms extracted from these data are also provided (inset). Bottom: H_2O_2 (pink) and DA (teal) traces centered around the onset of rotation (±1.0 s, vertical black box on color plot). (b) Top: representative color plot for the entire 300 s epoch from which the representative bout shown in (a) is extracted. Bottom: Concentration *vs* time traces. Periods of rotational behavior are shaded in gray. (c) Concentration traces from all rotational bouts (n = 15) averaged for this epoch from this individual animal. DA and H_2O_2 signals are negatively correlated around the initiation of contraversive rotational behavior (ρ = −0.9917, P < 0.0001), such that DA concentrations transiently decrease as H_2O_2 concentrations increase.

during dyskinetic behaviors in lesioned animals after 1 week of L-DOPA treatment (Figures 3b,d,h). There are many reports of increased DA in the ipsilateral striatum of dyskinetic rats, as measured using approaches including microdialysis sampling, PET imaging, and chronoamperometry.[14,38,39] Similar increases in striatal DA have been reported in human patients shortly after L-DOPA administration.[40] In the ipsilateral hemisphere, swings in DA concentration can result from altered monoamine transporter function[41] or from ectopic DA release (which can occur from serotonergic neurons[42] or even from non-neuronal cells[43,44]). These cells have the ability to synthesize DA from L-DOPA but lack the associated mechanisms to regulate its release. Thus, pulsatile neurochemical signals were anticipated.

The elevated H_2O_2 tone that was recorded in both striata of lesioned animals after 1 week of L-DOPA treatment was also not unexpected. H_2O_2 can be generated in the auto-oxidation of extracellular DA or its metabolites,[45] with the continued activation of the MSNs themselves (cellular respiration),[8,46] or through a glial neuroinflammatory response.[47] A recent study that used L-DOPA to elevate cytosolic DA in SNpc neurons demonstrated that DA metabolism results in the production of H_2O_2, specifically at the mitochondrial membrane. As such, H_2O_2 could be readily shuttled into the electron transport chain to drive ATP generation to meet the bioenergetic needs of sustained transmitter release as well as to potentially decrease ROS cytotoxicity.[46] The IR-MALDESI images suggest that the elevated H_2O_2 tone did not negatively impact the relative abundance of striatal DA remaining by week 3, because the extent of the DA depletion was not different from that in lesioned rats treated daily with saline (Figure 1), consistent with other studies.[13] Additionally, no bilateral differences in DA abundance were noted in intact animals. The elevated H_2O_2 tone was largely normalized after 3 weeks of treatment, but the mechanisms regulating this progressive change remain to be determined.

The data presented herein reveal striatal DA and H_2O_2 transients evident throughout the recording sessions, including in the absence of pronounced behavior. Animals typically exhibited a complex, inconsistent mix of AIMs (hyperkinetic, involuntary movements) or a short pause in behavior, followed by a sharp transition to rotation. H_2O_2 concentrations increased with the initiation of involuntary rotation, as DA concentrations simultaneously decreased at the same recording sites. However, it was only after 3 weeks of chronic L-DOPA administration that these neurochemical transients reliably correlated with the onset of contraversive rotational behavior (Figures 5 and 6; Video S1), suggesting an adaptive neurochemical response. We did not readily observe DA transients occurring with other motoric behaviors (Figure S2), but rather it was specific to rotation onset (Figure 6). It is entirely possible that DA concentrations increased with the onset of voluntary locomotion (*e.g.*, in controls), but this was not assessed as these subjects mostly rested. As such, the rapid, bilateral decrease in striatal DA and increase in H_2O_2 at

https://doi.org/10.1021/acsmeasuresciau.1c00030
ACS Meas. Sci. Au 2022, 2, 120−131

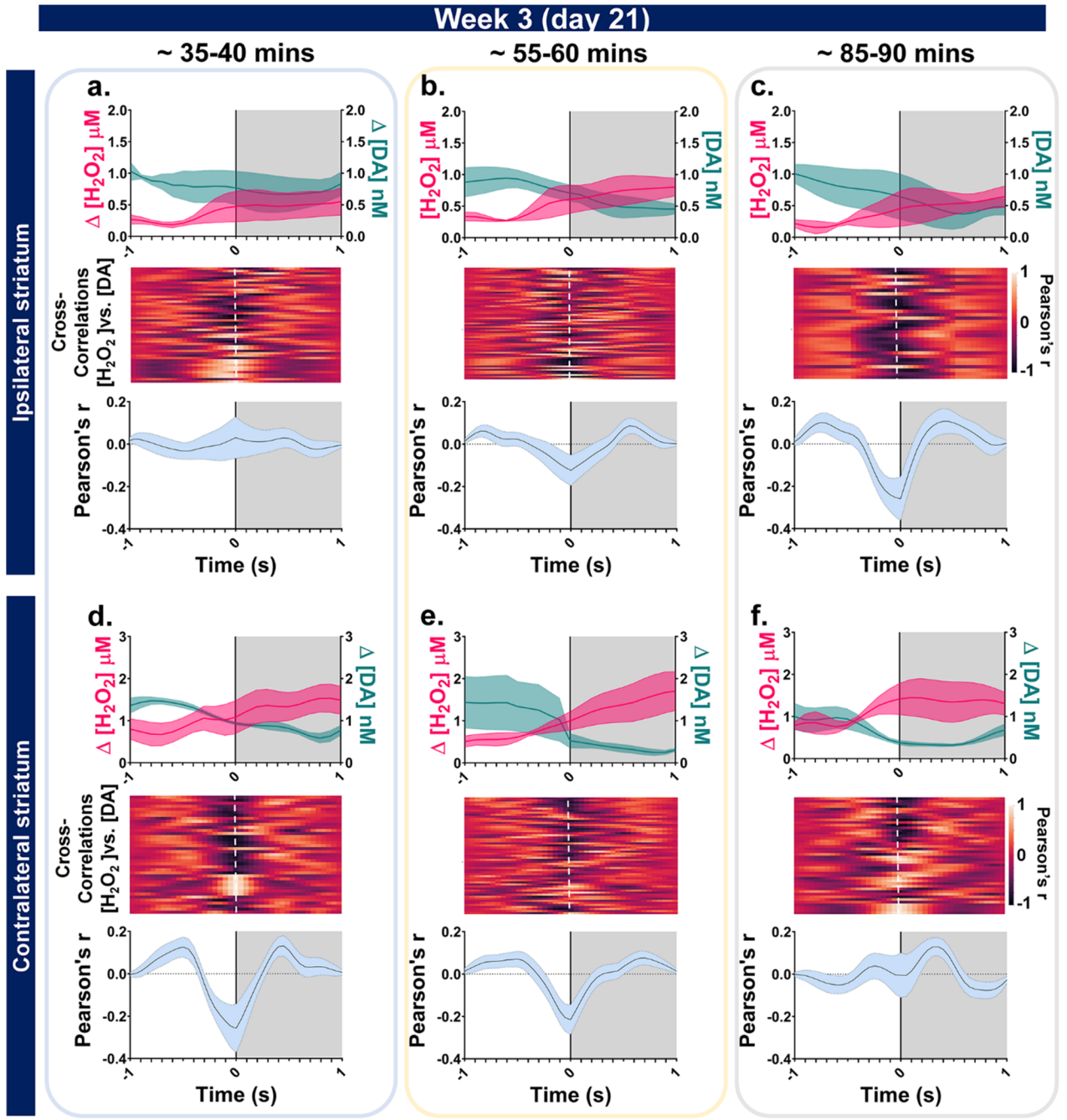

Figure 6. After 3 weeks of L-DOPA treatment, DA and H_2O_2 transients in the striatum are negatively correlated at the onset of contraversive rotational behavior. Top panels: DA concentrations decreased as H_2O_2 concentrations simultaneously increased. The signals were negatively correlated with one another around the onset of rotational behavior for all time points examined (n = 3 animals ipsilateral, n = 4 animals contralateral, ∼10−30 rotational bouts per each epoch in all animals; $P < 0.01$ for (a); $P < 0.0001$ for (b)−(f)). Middle panels: Cross correlations for each rotational bout are shown in the form of Pearson's R heat maps. Bottom panels: Average correlation coefficients.

rotation onset appears distinct to L-DOPA associated, contraversive, involuntary locomotion.

Several studies have demonstrated increased DA neuron activity with respect to the initiation of robust, voluntary locomotion.[2,48,49] However, measures of cell firing are not indicative of any specific neurochemical signaling per se, as cells release many substances. For instance, DA cells are known to release GABA[50] and glutamate,[51,52] and they express a variety of neuropeptides (for review, see refs 53 and 54), in addition to DA. DA burst firing is sufficient to produce striatal DA transients,[55] and DA release influences MSNs to generate a cascade of signaling through the motor loop that ultimately results in locomotion. The activation of MSNs produces membrane-permeable H_2O_2, which can suppress DA release by way of ATP-sensitive K^+ (K_{ATP}) channels on DA axons.[9,16,17,22] It is equally likely that H_2O_2 can diffuse to act at K_{ATP} channels located on serotonergic terminals or other nearby non-neuronal cells. This could suppress the ectopic release of L-DOPA-derived DA in the denervated striatum, as these channels are expressed on a multitude of cellular subtypes.[56]

Both dopamine D1 and D2 receptors are implicated in dyskinesias,[57,58] but activation of D1-receptor containing

https://doi.org/10.1021/acsmeasuresciau.1c00030
ACS Meas. Sci. Au 2022, 2, 120−131

MSNs (D1R-MSNs) is sufficient to induce dyskinetic behavior.[59,60] Indeed, *in vivo* photometry studies in genetically modified mice have shown transient increases in MSN activity that precede and predict (within 500 ms) the start of contraversive movements.[61] Furthermore, a recent study in mice has used the targeted recombination in active population (TRAP) strategy to demonstrate that a specific subset of striatal cells (mostly direct pathway D1R-MSNs) is reliably activated with dyskinetic behavior associated with L-DOPA.[15,60] Optogenetic activation of these TRAP-ed cells elicited AIMs *and* contraversive rotations.[15] Importantly, MSN activity is modulated by interneurons.[62] The phasic activity of striatal cholinergic interneurons has been shown to rapidly increase with the initiation of spontaneous voluntary movements in intact animals,[49] and striatal DA and acetylcholine are dysregulated in PD and with L-DOPA induced dyskinesias (for review, see ref 63). Thus, future studies should investigate the potential adaptive role of serotonergic inputs, subsets of MSNs, and cholinergic striatal interneurons on the initiation of involuntary rotational behaviors.

Here, we have directly shown that DA and H_2O_2 dynamics precisely correlate with the onset of *spontaneous* bouts of robust rotation induced by L-DOPA administration in hemiparkinsonian rats. The simultaneous voltammetric measurements of H_2O_2 and DA lend credence to the argument that dramatically fluctuating DA concentrations in the dorsal striatum may contribute to the development of L-DOPA-induced behavioral abnormalities, as suggested previously.[13,42] Notably, the data suggest a neuroadaptive response to L-DOPA treatment. As such, future studies that evaluate the effects of ROS and other principal neuromodulators on the specific subsets of cells implicated in dyskinesia will be critical. Such studies will continue to clarify the mechanisms that underlie debilitating dyskinetic side effects, and will ultimately aid in the development of improved therapeutic strategies for PD.

MATERIALS AND METHODS

Chemicals

All chemicals were purchased from Millipore Sigma (St. Louis, MO) and used as received, unless otherwise specified. *In vitro* electrochemical experiments were carried out in 0.01 M phosphate buffered saline (PBS) at physiological pH 7.4. All aqueous solutions were made from double deionized water >18 MΩ·cm. L-3,4-Dihydroxyphenylalanine methyl ester (L-DOPA) and benserazide hydrochloride were dissolved in sterile saline (0.9% NaCl; Hospira, Lake Forest, IL).

For IR-MALDESI experiments, HPLC-grade methanol and water were purchased from Burdick & Jackson (Muskegon, MI). Formic acid was obtained from Sigma-Aldrich (St. Louis, MO). Nitrogen gas (purity ≥ 99.99%) used for purging the IR-MALDESI imaging enclosure was purchased from Arc3 Gases (Raleigh, NC).

Electrode Fabrication

Fused-silica tubing (75 μm outer diameter/18 μm inner diameter) with a polyimide coating (Molex, Lisle, IL) was cut to 10 mm in length and placed in a bath of 70% isopropyl alcohol. A T-650/35 polyacrylonitrile carbon fiber (7 μm diameter, Cytec Industries, West Patterson, NJ) was inserted into the tubing under a stereoscopic microscope. The carbon fiber and silica were allowed to dry for 24 h. A seal was created at one end of the silica tubing using fast hardening 5 min epoxy (McMaster Carr, Atlanta, GA). An electrical connection with the carbon fiber was made using conductive silver epoxy (MG Chemical, Thief River Falls, MN) and a gold pin (Newark Element 14, Palatine, IL). This was allowed to dry for at least 24 h. The connection was insulated using fast curing epoxy and the electrodes were subsequently placed in a 105 °C oven for 20 min to allow the epoxy to cure. The connection was insulated a second time with GC Electronics Insulating Coating (GC Electronics, Rockford, IL). The exposed carbon fibers were cut to ∼100 μm under a stereoscopic microscope. Thereafter, carbon-fiber microelectrodes were electrochemically conditioned *in vitro* and the shape of the background signal was inspected prior to implantation.

The Ag/AgCl reference electrodes were made using 0.25 mm silver wire. A connection was made using a gold pin, and heat shrink was used to insulate it. The silver wire and gold pin were positioned through a hollowed MD 2250 guide cannula stylet cap (BASi Instruments, West Lafayette, IN), and a 5 min epoxy was used to secure it in place. The exposed wire was chloridized in 0.1 M HCl with the aid of a 9 V battery just prior to implantation on the day of each experiment.

Calibration

In vitro calibration of carbon-fiber microelectrodes was performed with a custom flow-injection apparatus in a home-built Faraday cage. The working electrodes were lowered into a custom electrochemical cell using a micromanipulator (World Precision Instruments, Inc., Sarasota, FL). Electrodes were conditioned by application of the voltammetric waveform (−0.4 to 1.4 V at a rate of 400 V/s), applied at 60 Hz for a minimum of 15 min, until the electrochemical background current stabilized. Data was subsequently collected at 10 Hz. A syringe pump (New Era Pump Systems, Inc., Wantagh, NY) supplied a continuous flow (1 mL/min) of PBS across both the working and reference (Ag/AgCl) electrodes. Bolus injections of analyte were introduced to the electrode surface using a six-port HPLC valve and air actuator controlled by a digital valve interface (Valco Instruments Co., Inc., Houston, TX). Calibrations of dopamine (DA), hydrogen peroxide (H_2O_2), and an acidic pH shifts were performed using 5 standards for physiological concentrations of DA (250−1000 nM), H_2O_2 (20−80 μM), and shifts in pH (0.05−0.20 pH units). Bolus injections of each concentration were performed in triplicate, and the peak oxidative current was averaged.

Animal Subjects and Care

Animal care and use was in complete accordance with the NC State University institutional guidelines (IACUC) and the NIH's *Guide for the Care and Use of Laboratory Animals*. Drug-naïve, male Sprague−Dawley rats (275−300 g, Charles River Laboratories, Raleigh, NC) were housed (paired until surgery, individually thereafter) on a 12:12 h light/dark cycle with free access to food and water. Unilateral 6-OHDA lesions of the left SNpc were completed by the vendor. The vendor verified the lesion with a 0.2 mg/kg subcutaneous apomorphine challenge 5−7 days after surgery that elicited at least 5 rotations/min over 5 min.

Stereotaxic Surgery

All animals were allowed to acclimate to the facility for several days prior to electrode placement. Rats were anesthetized with 4% isoflurane (Henry Schein, Dublin, OH), and isoflurane was maintained at 1.5−2.0% during surgery. Rats were positioned in a stereotaxic frame (Kopf Instrumentation; Tujunga, CA). A heating pad (Harvard Apparatus, Holliston, MA) was used to maintain body temperature at ∼37 °C. Holes for electrodes were drilled in the skull according to coordinates from the rat brain atlas of Paxinos and Watson.[64] The working electrode(s) were placed in the dorsal striatum (anteroposterior (AP) + 1.2 mm and mediolateral (ML) ± 2.0 mm relative to bregma; dorsoventral (DV) −5.0 mm relative to skull). A guide cannula (BASi Instruments, West Lafayette, IN) for the removable Ag/AgCl reference electrode, and a threaded tether anchor were placed in sites posterior to the chronic working electrode(s). The animals were allowed to recover for a minimum of 2 weeks before experiments commenced.

Experimental Design

Saline (0.6 mL/kg intraperitoneal (i.p.)) or L-DOPA (6 mg/kg L-DOPA + 12 mg/kg benserazide hydrochloride, i.p.) was administered daily for 21 days at approximately 14:00 h. Electrochemical data were

https://doi.org/10.1021/acsmeasuresciau.1c00030
ACS Meas. Sci. Au 2022, 2, 120−131

recorded and behavior was simultaneously monitored every 7 days during the 21 day drug treatment. Recordings consisted of a 10 min baseline prior to drug administration, after which the recording continued for an additional 185 min.

Electrochemical Measurements in Awake Animals

Awake, freely moving rats were placed into a custom-built (North Carolina State University, Chemistry Dept. Machine Shop, Raleigh, NC) Lexan acrylic (Piedmont Plastics, Raleigh, NC) behavioral chamber with a flat floor. The center of the behavioral chamber was a square with an area of 412.9 cm^2. The sides of the box were 57.6 cm high. The bottom 10.8 cm of each side was sloped at a 45° angle. The chamber was enclosed within a custom-built Faraday cage. A neuroelectrochemical headstage kit (24" cable) for current amplification (Pine research instrumentation, Durham, NC) was connected to a SwivElectra commutator (Crist instrument company, Hagerstown, MD) to allow unrestricted motion in the chamber. This was connected to a multichannel, custom-built instrument for potential application and current transduction (University of North Carolina at Chapel Hill, Department of Chemistry, Electronics Facility). A 6363 PCIe bus card (National Instruments Corp., Austin, TX) was used for waveform output. HDCV software (University of North Carolina at Chapel Hill, Department of Chemistry, Electronics Facility) controlled the waveform input and output. Signal processing (background subtraction, signal averaging and digital filtering (2-pole Sallen-Key Filter, 2 kHz)) was software controlled.

On the day of an electrochemical recording, a removable Ag/AgCl reference electrode was positioned into the guide cannula. The carbon-fiber microelectrodes were conditioned with the detection waveform applied at 60 Hz for at least 10 min and then at 10 Hz until they were stable over a 300 s time frame. Experimental data were then collected at 10 Hz. Four web cameras were controlled using iSpy Connect software version 6.0 to record behavior using TechSmith Camstasia software version 8.5. A BOB-4 video character generator (Decade Engineering, Turner, OR) was synchronized to the HDCV software to timestamp the electrochemical recording for precise correlation with the behavioral recording.

Quantification of Dyskinetic Behavior

The AIM rating score outlined by Lindgren and Lane[65] was used to quantify dyskinetic movements. Video-recorded behavior was scored by two researchers blind to treatment condition. The global AIM value for axial, orolingual, and limb dyskinesias was calculated by multiplying the amplitude score by the frequency score in 1 min time bins every 20th min of the 185 min recording session in week 1 (day 7) and week 3 (day 21). Rotations were quantified by counting the total number of full (360°) rotations every 21st min of these sessions.

Brain Slice Imaging Using Mass Spectrometry

IR-MALDESI coupled to a Q Exactive Plus (Thermo Scientific, Bremen, Germany) mass spectrometer was used to measure the spatial distribution of DA in rat brain slices. The details of home-built ambient ionization source have been described elsewhere.[23,24] Briefly, an infrared laser (2940 nm) was used to ablate neutral species from brain slices, followed by postionization in an orthogonally oriented electrospray plume.

Rats were deeply anesthetized with 4% isoflurane. After decapitation, brains were rapidly removed (<2 min) and quickly frozen with either liquid nitrogen (ARC3 Gases, Raleigh, NC) or a 2-methylbutane/dry ice bath (Millipore Sigma, St. Louis, MO). Biological samples were stored at −80 °C until the time of analysis. A thin layer of optimal cutting temperature (OCT) mounting medium (Scigen Scientific, Gardena, CA) was applied to a cryostat specimen disk. Samples were placed onto the OCT-coated specimen holder and thermally equilibrated for 10 min at −20 °C. The brains were sectioned using a Leica CM1950 cryomicrotome (Buffalo Grove, IL) and thaw mounted onto a precleaned microscope slide. High-profile, coated microtome blades were purchased from VWR (Batavia, IL). Tissue thickness varied from 25 to 100 μm, depending on tissue freshness. Fresh samples were easily cut at 25 μm, while older samples were sliced at 100 μm to ensure uniform slicing. Sample sectioning is one of the key steps in IR-MALDESI MSI, because every voxel (volumetric element corresponding to one image pixel) on a slice has to be positioned the same distance from the laser to ensure uniform sampling.

Slides were placed onto an XY translation stage and housed inside an acrylic enclosure with relative humidity lowered to ∼10% by purging with nitrogen gas. The stage temperature was lowered to −9 °C and held constant for 10 min to allow the tissue to reach thermal equilibrium. Next, the enclosure door was opened to increase humidity and to form a thin layer of ice on the tissue. The enclosure door was closed and relative humidity lowered to ∼10% to prevent further ice formation during imaging. When humidity stabilized, a 2940 nm laser (JGM Associates, INC., Burlington, MA) was used to ablate material from the sample with two mid-IR laser pulses. Spot-to-spot spacing varied: 200 × 200, 250 × 200, and 150 × 150 μm^2. ESI flow rate also varied from 1 to 2 μL/min.

A solution of 0.2% formic acid in 50:50 (v/v) methanol/water was used as the ESI solvent. In positive ESI mode, DA was readily evidenced as an $[M + H^+]^+$ ion. Since IR-MALDESI is a pulsed ionization source, the automatic gain control function was disabled and the injection time was set to 75 ms. All spectra were generated at a resolving power of 140 000_{fwhm} at m/z 200 within an m/z range of 100−400. To achieve a low mass measurement accuracy, peaks of phthalic anhydride (m/z 149.0233 $[M + H^+]^+$), polysiloxane (m/z 371.1012 $[M + H^+]^+$), and diisooctyl phthalate (m/z 391.2843 $[M + H^+]^+$ and 413.2662 $[M + Na^+]^+$) were used as lock-masses for internal calibration. Following MSI analysis, each slice was stained using Histogene staining solution (Thermo Fisher Scientific, Carlsbad, CA). Optical images were acquired using a 10× objective on an LMD7000 (Leica, Buffalo Grove, IL).

The.RAW files generated by the Q Exactive Plus were processed in XCalibur software (version 2.2, Thermo Fisher Scientific, San Jose, CA) and then converted into .mzML format using the open-source MSConvertGUI tool from ProteoWizard. The .mzML files were then converted to .imzML files using the imzML converter tool. Th e.imzML files were finally loaded into MSiReader, an open-source MSI data analysis software developed at NC State, to produce ion abundance heat maps.

Data Analysis and Statistics

All plots are presented as mean ± SEM. Plots and statistics were done using GraphPad Prism 7.04 for Windows, with the exception of cross-correlations which were performed in Python version 3.7.6 using the Scipy package.[66] For this, the full discrete linear cross-correlation of the inputs, *i.e.*, either the H_2O_2 or DA concentration, was calculated between −1 and 1 s around a rotation onset in 0.1 s time steps (21 total time points per analyte). For all statistical tests, significance was determined using Sidak posthoc comparisons with $P < 0.05$.

Relative DA and H_2O_2 abundance were quantified in IR-MALDESI MSI images of lesioned *vs* intact striata using a two-way nonrepeated measures ANOVA with striatal hemisphere and treatment condition as factors. Linear regression was used to relate the extent of the lesion to abnormal behaviors. Global AIMs scores and 360° rotations were analyzed by three-way ANOVA (treatment condition (*i.e.*, lesioned L-DOPA *vs* pooled controls) × week × time) with repeated measures on time and week. When a significant three-way interaction occurred, two-way ANOVA with repeated measures on time and week was completed for the lesioned-L-DOPA animals for treatment week × time.

To analyze FSCV data, background currents were removed by subtraction of cyclic voltammograms recorded at the minimum current generated for each targeted species, within a given time window. DA and H_2O_2 tones were roughly assessed in 300 s bins collected every 20 min by integrating the area under the concentration *vs* time trace extracted from the voltammetric data. Signal that exceeded 3 times the standard deviation of the noise for at least 5 s was termed "tone" for a given analyte. Animal behavior and chemical tone were analyzed using ordinary two-way ANOVA. The sources of variance were treatment group and time, with Sidak posthoc comparison to lesioned L-DOPA treated animals.

https://doi.org/10.1021/acsmeasuresciau.1c00030
ACS Meas. Sci. Au 2022, 2, 120−131

Analysis of rapid (less than 5 s) chemical transients was performed using principal component regression (PCR), a multivariate statistical method for quantitative determination of individual chemical contributors to the data (HDCV Analysis Software, University of North Carolina at Chapel Hill, Department of Chemistry, Electronics Facility).[67] Training sets consisted of representative cyclic voltammograms for DA, H_2O_2, and pH collected *in vitro*. Linear regression was used to determine the slope (calibration factor). The threshold for the sum of the squares of the residuals (Q_α) was set at the 95% confidence level. Once individual concentration *vs* time traces were extracted, data were centered around the onset of contraversive rotational behavior (±1 s). Across this 2 s window, Spearman's correlation analyses were used to quantify the correlation between H_2O_2 and DA.

■ ASSOCIATED CONTENT

Supporting Information

The Supporting Information is available free of charge at https://pubs.acs.org/doi/10.1021/acsmeasuresciau.1c00030.

Additional data with respect to the quantitative analyses performed in this study (PDF)

Video that shows neurochemical dynamics correlated with rotational behavior in an awake hemiparkinsonian rat (MPG)

■ AUTHOR INFORMATION

Corresponding Author

Leslie A. Sombers − *Department of Chemistry and Comparative Medicine Institute, North Carolina State University, Raleigh, North Carolina 27695, United States;* orcid.org/0000-0002-0978-9795; Email: lasomber@ncsu.edu

Authors

Leslie R. Wilson − *Department of Chemistry, North Carolina State University, Raleigh, North Carolina 27695, United States*

Christie A. Lee − *Department of Chemistry, North Carolina State University, Raleigh, North Carolina 27695, United States*

Catherine F. Mason − *Department of Chemistry, North Carolina State University, Raleigh, North Carolina 27695, United States*

Sitora Khodjaniyazova − *Department of Chemistry, North Carolina State University, Raleigh, North Carolina 27695, United States*

Kevin B. Flores − *Department of Mathematics and Center for Research in Scientific Computation, North Carolina State University, Raleigh, North Carolina 27695, United States*

David C. Muddiman − *Department of Chemistry, Molecular Education, Technology, and Research Innovation Center (METRIC), and Center for Research in Scientific Computation, North Carolina State University, Raleigh, North Carolina 27695, United States;* orcid.org/0000-0003-2216-499X

Complete contact information is available at: https://pubs.acs.org/10.1021/acsmeasuresciau.1c00030

Author Contributions

#L.R.W. and C.A.L contributed equally to this work. L.R.W., C.A.L., C.F.M., and L.A.S. contributed to experimental design, electrochemical and behavioral data collection, and data analysis and interpretation. K.B.F. contributed to electrochemical and behavioral data analysis. S.K. and D.C.M. contributed to mass spectrometric data collection and analysis. All authors contributed to manuscript preparation.

Funding

This work was supported by the U.S. National Institutes of Neurological Disorders and Stroke (1R01NS076772-01 to L.A.S.) and the U.S. National Institutes of General Medical Sciences (5R01GM087964-07 to D.C.M.), the NCSU Office of Undergraduate Research (partial support of C.F.M.), and the NCSU Keck Center for Behavioral Biology (partial support of L.W.).

Notes

The authors declare no competing financial interest.
The authors do not have any unexpected or significant hazards or risks to report for this study.

■ ACKNOWLEDGMENTS

We would like to thank Dr. Xiaohu Xie for his help with data analysis, Karen Butler, Sambit Panda, and Nicolas Williams for assisting with electrochemical data collection, and Danielle Tucker for help with graphical design.

■ REFERENCES

(1) Blonder, L. X. Historical and cross-cultural perspectives on Parkinson's disease. *J. Complementary Integr. Med.* **2018**, *15*, 20160065.

(2) Howe, M. W.; Dombeck, D. A. Rapid signalling in distinct dopaminergic axons during locomotion and reward. *Nature* **2016**, *535*, 505−510.

(3) Smith, K. S.; Graybiel, A. M. Habit formation. *Dialogues Clin. Neurosci.* **2016**, *18*, 33−43.

(4) Howard, C. D.; Li, H.; Geddes, C. E.; Jin, X. Dynamic Nigrostriatal Dopamine Biases Action Selection. *Neuron* **2017**, *93*, 1436−1450.

(5) Jenner, P. Oxidative stress in Parkinson's disease. *Ann. Neurol.* **2003**, *53*, S26−S38.

(6) Schapira, A. H.; et al. Mitochondrial complex I deficiency in Parkinson's disease. *J. Neurochem.* **1990**, *54*, 823−827.

(7) Schober, A. Classic toxin-induced animal models of Parkinson's disease: 6-OHDA and MPTP. *Cell Tissue Res.* **2004**, *318*, 215−224.

(8) Chinta, S. J.; Andersen, J. K. Redox imbalance in Parkinson's disease. *Biochim. Biophys. Acta, Gen. Subj.* **2008**, *1780*, 1362−1367.

(9) Avshalumov, M. V.; Chen, B. T.; Koos, T.; Tepper, J. M.; Rice, M. E. Endogenous hydrogen peroxide regulates the excitability of midbrain dopamine neurons via ATP-sensitive potassium channels. *J. Neurosci.* **2005**, *25*, 4222−4231.

(10) Hauser, R. A. Levodopa: past, present, and future. *Eur. Neurol.* **2009**, *62*, 1−8.

(11) Manson, A.; Stirpe, P.; Schrag, A. Levodopa-induced-dyskinesias clinical features, incidence, risk factors, management and impact on quality of life. *J. Parkinson's Dis.* **2012**, *2*, 189−198.

(12) Zigmond, M. J.; Abercrombie, E. D.; Berger, T. W.; Grace, A. A.; Stricker, E. M. Compensations after lesions of central dopaminergic neurons: some clinical and basic implications. *Trends Neurosci.* **1990**, *13*, 290−296.

(13) Carta, M.; et al. Role of striatal L-DOPA in the production of dyskinesia in 6-hydroxydopamine lesioned rats. *J. Neurochem.* **2006**, *96*, 1718−1727.

(14) Lindgren, H. S.; Andersson, D. R.; Lagerkvist, S.; Nissbrandt, H.; Cenci, M. A. L-DOPA-induced dopamine efflux in the striatum and the substantia nigra in a rat model of Parkinson's disease: temporal and quantitative relationship to the expression of dyskinesia. *J. Neurochem.* **2010**, *112*, 1465−1476.

(15) Girasole, A. E.; et al. A Subpopulation of Striatal Neurons Mediates Levodopa-Induced Dyskinesia. *Neuron* **2018**, *97*, 787−795.

(16) Avshalumov, M. V.; Patel, J. C.; Rice, M. E. AMPA Receptor-Dependent H2O2 Generation in Striatal Medium Spiny Neurons But Not Dopamine Axons: One Source of a Retrograde Signal That Can Inhibit Dopamine Release. *J. Neurophysiol.* **2008**, *100*, 1590−1601.
(17) Patel, J. C.; Witkovsky, P.; Coetzee, W. A.; Rice, M. E. Subsecond regulation of striatal dopamine release by pre-synaptic KATP channels. *J. Neurochem.* **2011**, *118*, 721−736.
(18) Robinson, D. L.; Heien, M. L.; Wightman, R. M. Frequency of dopamine concentration transients increases in dorsal and ventral striatum of male rats during introduction of conspecifics. *J. Neurosci.* **2002**, *22*, 10477−10486.
(19) Phillips, P. E.; Stuber, G. D.; Heien, M. L.; Wightman, R. M.; Carelli, R. M. Subsecond dopamine release promotes cocaine seeking. *Nature* **2003**, *422*, 614−618.
(20) Roitman, M. F.; Stuber, G. D.; Phillips, P. E.; Wightman, R. M.; Carelli, R. M. Dopamine operates as a subsecond modulator of food seeking. *J. Neurosci.* **2004**, *24*, 1265−1271.
(21) Day, J. J.; Roitman, M. F.; Wightman, R. M.; Carelli, R. M. Associative learning mediates dynamic shifts in dopamine signaling in the nucleus accumbens. *Nat. Neurosci.* **2007**, *10*, 1020−1028.
(22) Spanos, M.; et al. Quantitation of hydrogen peroxide fluctuations and their modulation of dopamine dynamics in the rat dorsal striatum using fast-scan cyclic voltammetry. *ACS Chem. Neurosci.* **2013**, *4*, 782−789.
(23) Caleb Bagley, M.; Garrard, K. P.; Muddiman, D. C. The development and application of matrix assisted laser desorption electrospray ionization: The teenage years. *Mass Spectrom. Rev.* **2021**, DOI: 10.1002/mas.21696.
(24) Pace, C. L.; Horman, B.; Patisaul, H.; Muddiman, D. C. Analysis of neurotransmitters in rat placenta exposed to flame retardants using IR-MALDESI mass spectrometry imaging. *Anal. Bioanal. Chem.* **2020**, *412*, 3745−3752.
(25) Lundblad, M.; et al. Pharmacological validation of behavioural measures of akinesia and dyskinesia in a rat model of Parkinson's disease. *Eur. J. Neurosci* **2002**, *15*, 120−132.
(26) Marin, C.; Rodriguez-Oroz, M. C.; Obeso, J. A. Motor complications in Parkinson's disease and the clinical significance of rotational behavior in the rat: have we wasted our time? *Exp. Neurol.* **2006**, *197*, 269−274.
(27) Bibbiani, F.; Costantini, L. C.; Patel, R.; Chase, T. N. Continuous dopaminergic stimulation reduces risk of motor complications in parkinsonian primates. *Exp. Neurol.* **2005**, *192*, 73−78.
(28) Lindgren, H. S.; Rylander, D.; Ohlin, K. E.; Lundblad, M.; Cenci, M. A. The "motor complication syndrome" in rats with 6-OHDA lesions treated chronically with L-DOPA: relation to dose and route of administration. *Behav. Brain Res.* **2007**, *177*, 150−159.
(29) Cenci, M. A.; Lindgren, H. S. Advances in understanding L-DOPA-induced dyskinesia. *Curr. Opin. Neurobiol.* **2007**, *17*, 665−671.
(30) Heikkila, R. E.; Shapiro, B. S.; Duvoisin, R. C. The relationship between loss of dopamine nerve terminals, striatal [3H]spiroperidol binding and rotational behavior in unilaterally 6-hydroxydopamine-lesioned rats. *Brain Res.* **1981**, *211*, 285−292.
(31) Hefti, F.; Melamed, E.; Sahakian, B. J.; Wurtman, R. J. Circling behavior in rats with partial, unilateral nigro-striatal lesions: effect of amphetamine, apomorphine, and DOPA. *Pharmacol., Biochem. Behav.* **1980**, *12*, 185−188.
(32) Miller, D. W.; Abercrombie, E. D. Role of high-affinity dopamine uptake and impulse activity in the appearance of extracellular dopamine in striatum after administration of exogenous L-DOPA: studies in intact and 6-hydroxydopamine-treated rats. *J. Neurochem.* **1999**, *72*, 1516−1522.
(33) Cenci, M. A.; Konradi, C. Maladaptive striatal plasticity in L-DOPA-induced dyskinesia. *Prog. Brain Res.* **2010**, *183*, 209−233.
(34) Papa, S. M.; Engber, T. M.; Kask, A. M.; Chase, T. N. Motor fluctuations in levodopa treated parkinsonian rats: relation to lesion extent and treatment duration. *Brain Res.* **1994**, *662*, 69−74.
(35) Stocchi, F. The levodopa wearing-off phenomenon in Parkinson's disease: pharmacokinetic considerations. *Expert Opin. Pharmacother.* **2006**, *7*, 1399−1407.
(36) Abercrombie, E. D.; Bonatz, A. E.; Zigmond, M. J. Effects of L-dopa on extracellular dopamine in striatum of normal and 6-hydroxydopamine-treated rats. *Brain Res.* **1990**, *525*, 36−44.
(37) Walker, M. D.; et al. Measuring dopaminergic function in the 6-OHDA-lesioned rat: a comparison of PET and microdialysis. *EJNMMI Res.* **2013**, *3*, 69.
(38) Carta, M.; Bezard, E. Contribution of pre-synaptic mechanisms to L-DOPA-induced dyskinesia. *Neuroscience* **2011**, *198*, 245−251.
(39) Lundblad, M.; et al. Chronic intermittent L-DOPA treatment induces changes in dopamine release. *J. Neurochem.* **2009**, *108*, 998−1008.
(40) de la Fuente-Fernandez, R.; et al. Levodopa-induced changes in synaptic dopamine levels increase with progression of Parkinson's disease: implications for dyskinesias. *Brain* **2004**, *127*, 2747−2754.
(41) Huot, P.; Fox, S. H.; Brotchie, J. M. Monoamine reuptake inhibitors in Parkinson's disease. *Parkinson's Dis.* **2015**, *2015*, 609428.
(42) Carta, M.; Bjorklund, A. The serotonergic system in L-DOPA-induced dyskinesia: pre-clinical evidence and clinical perspective. *J. Neural Transm. (Vienna)* **2018**, *125*, 1195.
(43) Carta, A. R.; et al. l-DOPA-induced dyskinesia and neuro-inflammation: do microglia and astrocytes play a role? *Eur. J. Neurosci* **2017**, *45*, 73−91.
(44) Melamed, E.; Hefti, F.; Wurtman, R. J. Nonaminergic striatal neurons convert exogenous L-dopa to dopamine in parkinsonism. *Ann. Neurol.* **1980**, *8*, 558−563.
(45) Lipski, J.; et al. L-DOPA: a scapegoat for accelerated neurodegeneration in Parkinson's disease? *Prog. Neurobiol.* **2011**, *94*, 389−407.
(46) Graves, S. M.; et al. Dopamine metabolism by a monoamine oxidase mitochondrial shuttle activates the electron transport chain. *Nat. Neurosci.* **2020**, *23*, 15−20.
(47) Soliman, M. K.; Mazzio, E.; Soliman, K. F. Levodopa modulating effects of inducible nitric oxide synthase and reactive oxygen species in glioma cells. *Life Sci.* **2002**, *72*, 185−198.
(48) da Silva, J. A.; Tecuapetla, F.; Paixão, V.; Costa, R. M. Dopamine neuron activity before action initiation gates and invigorates future movements. *Nature* **2018**, *554*, 244−248.
(49) Howe, M.; et al. Coordination of rapid cholinergic and dopaminergic signaling in striatum during spontaneous movement. *eLife* **2019**, *8*, No. e44903.
(50) Tritsch, N. X.; Ding, J. B.; Sabatini, B. L. Dopaminergic neurons inhibit striatal output through non-canonical release of GABA. *Nature* **2012**, *490*, 262−266.
(51) Chuhma, N. Dopamine neuron glutamate cotransmission evokes a delayed excitation in lateral dorsal striatal cholinergic interneurons. *eLife* **2018**, *7*, e39786.
(52) Eskenazi, D.; et al. Dopamine Neurons That Cotransmit Glutamate, From Synapses to Circuits to Behavior. *Front. Neural Circuits* **2021**, *15*, 665386.
(53) Trudeau, L.-E.; et al. The multilingual nature of dopamine neurons. *Prog. Brain Res.* **2014**, *211*, 141−164.
(54) Morales, M.; Margolis, E. B. Ventral tegmental area: cellular heterogeneity, connectivity and behaviour. *Nat. Rev. Neurosci.* **2017**, *18*, 73−85.
(55) Sombers, L. A.; Beyene, M.; Carelli, R. M.; Wightman, R. M. Synaptic overflow of dopamine in the nucleus accumbens arises from neuronal activity in the ventral tegmental area. *J. Neurosci.* **2009**, *29*, 1735−1742.
(56) Dunn-Meynell, A. A.; Rawson, N. E.; Levin, B. E. Distribution and phenotype of neurons containing the ATP-sensitive K+ channel in rat brain. *Brain Res.* **1998**, *814*, 41−54.
(57) Castela, I.; Hernandez, L. F. Shedding light on dyskinesias. *Eur. J. Neurosci* **2021**, *53*, 2398−2413.
(58) Kiessling, C. Y.; Lanza, K.; Feinberg, E.; Bishop, C. Dopamine receptor cooperativity synergistically drives dyskinesia, motor

behavior, and striatal GABA neurotransmission in hemiparkinsonian rats. *Neuropharmacology* **2020**, *174*, 108138.
(59) Perez, X. A.; Zhang, D.; Bordia, T.; Quik, M. Striatal D1 medium spiny neuron activation induces dyskinesias in parkinsonian mice. *Mov. Disord.* **2017**, *32*, 538−548.
(60) Ryan, M. B.; Bair-Marshall, C.; Nelson, A. B. Aberrant Striatal Activity in Parkinsonism and Levodopa-Induced Dyskinesia. *Cell Rep.* **2018**, *23*, 3438−3446.
(61) Cui, G.; et al. Concurrent activation of striatal direct and indirect pathways during action initiation. *Nature* **2013**, *494*, 238−242.
(62) Gritton, H. J.; et al. Unique contributions of parvalbumin and cholinergic interneurons in organizing striatal networks during movement. *Nat. Neurosci.* **2019**, *22*, 586−597.
(63) Conti, M. M.; Chambers, N.; Bishop, C. A new outlook on cholinergic interneurons in Parkinson's disease and L-DOPA-induced dyskinesia. *Neurosci. Biobehav. Rev.* **2018**, *92*, 67−82.
(64) Paxinos, G.; Watson, C. *The rat brain in stereotaxic coordinates: The new coronal set*, 5th ed.; Elsevier Academic, 2005.
(65) Lindgren, H. S.; Lane, E. L. Rodent Models of L-DOPA-Induced Dyskinesia. *Neuromethods* **2011**, *61*, 337−351.
(66) Virtanen, P.; et al. SciPy 1.0: fundamental algorithms for scientific computing in Python. *Nat. Methods* **2020**, *17*, 261−272.
(67) Rodeberg, N. T.; et al. Construction of Training Sets for Valid Calibration of in Vivo Cyclic Voltammetric Data by Principal Component Analysis. *Anal. Chem.* **2015**, *87*, 11484−11491.

https://doi.org/10.1021/acsmeasuresciau.1c00030
ACS Meas. Sci. Au 2022, 2, 120−131